DOI: 10.32615/ps.2020.023 PHOTOSYNTHETICA 58 (3): 790-798, 2020

# Photosynthetic $CO_2$ response to soil water and its simulation using different models in leaves of two species

Q. WU[*,**], T. ZHANG[***], C.R. LI[#,##,+], H.B. XIE[****], and G.C. ZHANG[***]

*School of Art, Shangdong Jianzhu University, 250101 Jinan, China*[*]
*Editorial Department of Journal, Shandong Jianzhu University, 250101 Jinan, China*[**]
*Faculty of Forestry, Shandong Agricultural University, 271018 Tai'an, China*[***]
*The Forestry Science and Technology Training Center of Shandong, 250013 Jinan, China*[****]
*Taishan Forest Ecosystem Research Station, 271018 Tai'an, China*[#]
*Key Laboratory of State Forestry Administration for Silviculture of the Lower Yellow River, 271018 Tai'an, China*[##]

## Abstract

$CO_2$ concentrations and soil moisture conditions are important factors in photosynthesis of trees. This study investigated the photosynthetic $CO_2$ responses in the leaves of *Prunus sibirica* L. and *Pinus tabulaeformis* Carr. under eight soil water conditions in a semiarid loess hilly region. $CO_2$-response curves and physiological parameters were fitted using a rectangular hyperbola model, nonrectangular hyperbola model, exponential equation, and modified rectangular hyperbola model. Results revealed the relative soil water content (RWCs) for *P. sibirica* required to maintain higher photosynthetic rate ranging from 46.5 to 81.6%, and that for *P. tabulaeformis* ranging from 35.4 to 84.5%. When RWCs exceeded these ranges, the net photosynthetic rate of both species decreased. $CO_2$-response curves and three parameters, carboxylation efficiency, $CO_2$-compensation point, and photorespiration rate, were well fitted by the four models when RWCs was appropriate for *P. sibirica* and *P. tabulaeformis*. When RWCs exceeded the optimal ranges, only the modified rectangular hyperbola model could precisely simulate the $CO_2$-response curves and photosynthetic parameters of both species.

*Additional key words:* $CO_2$-response models; model simulation effect; photosynthetic $CO_2$ response; tree species.

## Introduction

Plant photosynthesis is a complex process affected greatly by $CO_2$ concentrations and soil moisture conditions (Drake *et al.* 2017, Guan *et al.* 2018). Soil moisture affects plant growth and development severely (Karimi *et al.* 2018, Bhusal *et al.* 2019), as well as limits plant photosynthesis through carbon metabolism (Bellasio *et al.* 2018, Wang *et al.* 2019). However, plants display adaptability and resistance to water deficits (Renninger *et al.* 2014, Falqueto *et al*. 2017). Moreover, in a certain range of soil moisture, higher photosynthetic efficiency is related to plant species and their photosynthetic mechanism (Xia *et al.* 2016, Liu and Luo 2019). $CO_2$ is the substrate of photosynthesis, and its atmospheric concentration is predicted to reach ~ 700 µmol $mol^{-1}$ by the end of the century (IPCC 2013, Ha *et al.* 2019). Global water shortages are exacerbated by changes of increasing $CO_2$ concentrations and climate warming (Reich *et al.* 2018, Brito *et al.* 2019). The increase of $CO_2$ causes global climate change and directly affects plant metabolism and growth (Davidson *et al.* 2016, Jin *et al.* 2019). Photosynthetic $CO_2$ response is an important part of plant physiology and ecology research, and its measurement and simulation are the main ways to study plant photosynthesis. $CO_2$-response model has played an important role in increasing our understanding of photosynthetic carbon uptake, which has thereby improved our understanding and predictions of plant photosynthetic physiology and its response to environmental changes and biogeochemical systems (Nickelsen 2015, Liang and Liu 2017). $CO_2$-response curves can reflect the quantitative relationship between plant photosynthetic rate and $CO_2$ concentration, and can be used to estimate photosynthetic parameters, such as the maximum net photosynthetic rate ($P_{Nmax}$) and $CO_2$-saturation point ($C_{isat}$) (Sun *et al.* 2014, Niinemets *et al.* 2015).

$CO_2$-response process and parameters have been fitted using biochemical models (Farquhar *et al.* 1980), empirical models (Wang *et al.* 2012, von Caemmerer 2013), and optimized models (Ali *et al.* 2016, Liu *et al.* 2019b) based on biochemical models. Biochemical models can calculate two key parameters, the maximum rate of carboxylation ($V_{cmax}$) and the maximum electron transport rate ($J_{max}$) (King *et al.* 2012, Walker *et al.* 2017). Empirical

*Received* 19 November 2019, *accepted* 4 March 2020.
[+]Corresponding author; e-mail: chrli@sdau.edu.cn
*Abbreviations*: CE – carboxylation efficiency; $C_i$ – intercellular $CO_2$ concentration; $C_{isat}$ – $CO_2$-saturation point; FC – field water capacity; $J_{max}$ – maximum electron transport rate; MWC – mass water content; $P_N$ – net photosynthetic rate; $P_{Nmax}$ – maximum net photosynthetic rate; $R_p$ – photorespiration rate; RWCs – relative soil water content; $V_{cmax}$ – maximum carboxylation rate; $\Gamma$ – $CO_2$-compensation point.
*Acknowledgements*: This study was supported by the Doctoral Research Fund of Shandong Jianzhu University (XNBS1420), Shandong Agricultural Science and Technology (Forestry Science and Technology Innovation) fund project (2019LY005), and the National Natural Science Foundation of China (31570705). Q. Wu and T. Zhang contributed equally to this work.

models include the Michaelis-Menten model (Harley *et al.* 1992), rectangular hyperbola model (Baly 1935), nonrectangular hyperbola model (Wang *et al.* 2012), and exponential equation (Watling *et al.* 2000), which have been applied in most crops (Singh and Reddy 2016, Bellasio 2019) and some woody species (Groenendijk *et al.* 2011, Ellsworth *et al.* 2015). Ye (2010) thought the Michaelis-Menten and rectangular hyperbola models were essentially the same. In recent years, some studies have proposed the modified rectangular hyperbola model, an improved rectangular hyperbola model (Ye and Gao 2009, Ye and Yu 2009). This model has been applied to some gramineous plants (Kang *et al.* 2014, Ye *et al.* 2017, 2018), other herbs (Hu *et al.* 2008, Ye and Gao 2008), and some woody plants (Jiao and Wei 2010, Lv *et al.* 2016). Results revealed that this new model could overcome the limitations of traditional models fitting the $CO_2$-response curve and its characteristic parameters accurately. Previous studies on photosynthetic $CO_2$-response models mostly focused on the estimation and optimization of key parameters in field crops (Dubois *et al.* 2007, Sharkey 2016). However, the applicability of different models simulating the $CO_2$-response data of tree species under different soil water conditions has been rarely reported.

*P. sibirica* and *P. tabulaeformis* are common afforestation species in the arid and semiarid regions of Northern China, which have high economic value and play an important role in ecological restoration and soil and water conservation (Wang *et al.* 2015). *P. sibirica* is a broadleaf, deciduous tree species that is part of the *Rosaceae* family and is resistant to barren and dry conditions (Liu *et al.* 2019a). *P. tabulaeformis* is evergreen and timber tree species of Pinaceae, heliophilous and deep-rooted (Wang *et al.* 2015). In recent years, studies have focused on the growth (Bao 2015, Guo *et al*. 2017), water transpiration (Liu *et al*. 2015, Lu *et al.* 2017), and photosynthetic light-response characteristics (Lang *et al.* 2013, Wu *et al.* 2019) under different soil moisture conditions, while continuous observation and the examination of photosynthetic $CO_2$ response have not been addressed at many soil moisture gradients during the accelerated soil drought process. Therefore, the quantitative relationship between the photosynthetic $CO_2$-response process and soil moisture remains unclear.

In this study using potted seedlings of *P. sibirica* and *P. tabulaeformis*, $CO_2$-response curves and parameters were evaluated and fitted with the rectangular hyperbola model, nonrectangular hyperbola model, exponential equation, and modified rectangular hyperbola model under different soil moisture conditions. The goals of this study were to define the quantitative relationship between photosynthetic $CO_2$-response processes and soil moisture, as well as explore the applicability of different $CO_2$-response models to fit $CO_2$-response processes and parameters in leaves of two species. The findings of this study will provide an in-depth understanding of the photosynthetic characteristics and cultivation of two species in the loess hilly-gully region of Northern China. Furthermore, the applicability of different $CO_2$-response models can be evaluated from these findings and used in future studies.

## Materials and methods

**Study area**: The experimental site was located in the Tuqiaogou watersheds (37°36'58"N, 110°02'55"E) of Yukou Town, Fangshan County, Shanxi Province, China, a portion of the gully-hilly area of the Loess Plateau in the middle reaches of the Yellow River, which has a subarid, warm temperate, continental monsoon climate. The average annual precipitation is 525.0 mm with more than 70% of the precipitation concentrated between July and September. The annual potential evaporation is 1,839.7 mm with the greatest amount of evaporation occurring between April and June. The annual frost-free period lasts 140 d. The soil is classified as medium loessial soil, and the soil texture is uniform with a pH value ranging from 8.0 to 8.4. Vegetation consists mainly of trees, shrubs, lianas, and subshrubs. Tree species are predominantly *Robinia pseudoacacia*, *Platycladus orientalis*, *Syringa oblata*, and *Ulmus pumila*. Shrubs are mainly *Ulmus macrocarpa* and *Rosa xanthina*. Herbs consist of Compositae and Gramineae. Most of the forest land is sparse, and the stand stability is poor.

**Materials and water treatments**: Two-year-old *P. sibirica* and *P. tabulaeformis* were used as the experimental materials and were selected carefully to ensure consistency in their height, diameter, and growth. Plants were investigated and marked one by one before transplantation. In March 2018, seedlings were transplanted in containers (50 cm in height, 35 cm in diameter) with drainage holes in the bottom. Six basins with one plant in each pot were used. RWCs and photosynthetic $CO_2$ responses were determined in the leaves of two species in August. Three strong plants were selected and watered to saturation, and the initial RWCs was obtained; the first $CO_2$ response was also determined. Then, soil moisture gradients were obtained every 2 d through the natural water consumption method after artificially supplying water. The soil mass water content (MWC) was measured by the stoving method (Heyam 2012). The RWCs was considered as the ratio of MWC to the field water capacity (FC). The potting soil FC was roughly 24.3%, and the soil bulk density was 1.26 ± 0.13 g cm$^{-3}$. Eight RWCs gradients of *P. sibirica* were obtained, *i.e.*, 92.3, 81.6, 66.8, 53.7, 46.5, 35.7, 26.2, and 21.5%; that of *P. tabulaeformis* were 92.6, 84.5, 73.7, 56.8, 44.9, 35.4, 26.9, and 22.1%. The experiment was carried out under a canopy covered with plastic film in rainy days to prevent rain from interfering with RWCs.

**$CO_2$-response determination**: Three strong, mature leaves of two species were selected and marked. $CO_2$-response curves were measured using a *CIRAS-2* (*PP Systems*, Amesbury, MA, USA) portable photosynthesis system under different soil moisture conditions. The light-saturation point for *P. sibirica* was 1,200 μmol(photon) m$^{-2}$ s$^{-1}$ (Lang *et al.* 2013), while that of *P. tabulaeformis* was 1,300 μmol(photon) m$^{-2}$ s$^{-1}$ (Wu *et al.* 2019). Measurements were obtained under each soil moisture condition on separate days. The time of measurements lasted from 08:30 to 11:00 h in completely clear weather to reduce the effects of outside light fluctuations. The atmospheric temperature ranged from 24 to 26°C, and the relative humidity was approximately 60 ± 5.0%. $CO_2$ concentration in the leaf chamber was controlled and regulated from 0 to 1,400 µmol mol$^{-1}$ by a small cylinder with high $CO_2$. The $CO_2$ concentration gradients were 1,400; 1,200; 1,000; 800, 600, 400, 200, 180, 150, 120, 90, 60, 30, and 0 µmol mol$^{-1}$. The measurement lasted 120 s at each $CO_2$ concentration, and the apparatus automatically recorded the photosynthetic physiological parameters, including $P_N$ and intercellular $CO_2$ concentration ($C_i$).

**Data analysis**: $CO_2$-response curves were drawn with $C_i$ as the horizontal axis and $P_N$ as the vertical axis. According to the trends of measured data point, $C_{isat}$, $P_{Nmax}$, and Γ were estimated and regarded as measured values. Using the traditional linear regression method, $CE_0$, the carboxylation efficiency at $C_i = 0$, $CE_\Gamma$, the carboxylation efficiency at $C_i = \Gamma$, $CE_{\Gamma 0}$, the slope of the line between $C_i = 0$ and $C_i = \Gamma$, and $R_p$ were calculated, and used as the measured values to compare to the fitted values of the four models.

Statistical analyses were performed using *Microsoft Excel 2003* (*Microsoft Corp.*, Redmond, WA, USA). Significant differences were analyzed by a one-way analysis of variance (*ANOVA*) and *Duncan*'s post-hoc test. Nonlinear regression was analyzed using *SPSS v. 18.0* (*IBM Corp.*, Chicago, IL, USA). All of the measurements were performed three times; the means and calculated standard deviations (SD) were reported. Significant differences between $CO_2$-response parameters were interpreted at the level of 0.05 ($p$=0.05). The $CO_2$-response curve was fitted using the rectangular hyperbola model, nonrectangular hyperbola model, exponential equation, and modified rectangular hyperbola model.

**The rectangular hyperbola model** is expressed as follows (Baly 1935):

$$P_N(C_i) = \frac{\alpha P_{Nmax} C_i}{\alpha C_i + P_{Nmax}} - R_p \quad (1)$$

where α is the slope of the $CO_2$-response curve when $C_i = 0$ (namely, the initial slope of the $CO_2$-response curve, also called the initial CE).

$CE_\Gamma$, $CE_0$, and $CE_{\Gamma 0}$ can be calculated by:

$$CE_\Gamma = P_N'(C_i = \Gamma) = \frac{\alpha P_{Nmax}^2}{(\alpha\Gamma + P_{Nmax})^2} \quad (2)$$

$$CE_0 = P_N'(C_i = 0) = \alpha \quad (3)$$

$$CE_{\Gamma 0} = |R_p/\Gamma| \quad (4)$$

Γ can be obtained by:

$$\Gamma = \frac{R_p P_{Nmax}}{\alpha(P_{Nmax} - R_p)} \quad (5)$$

where the line y = $P_{Nmax}$ intersects the approximately straight line of $CO_2$-response curve when $C_i$ is below 200 µmol mol$^{-1}$, and the value of the intersected point on the $x$-axis is $C_{isat}$ (Wang *et al.* 2005).

**The nonrectangular hyperbola model** is expressed as follows (Wang *et al.* 2012):

$$P_N(C_i) = \frac{\alpha C_i + P_{Nmax} - \sqrt{(\alpha C_i + P_{Nmax})^2 - 4\alpha k C_i P_{Nmax}}}{2k} - R_p \quad (6)$$

where $k$ is the curved angle of the nonrectangular hyperbola; the definitions of other parameters are the same as above.

$CE_\Gamma$, $CE_0$, and $CE_{\Gamma 0}$ are as follows:

$$CE_\Gamma = P_N'(C_i = \Gamma) = \frac{\alpha}{2k}\left[1 - \frac{(\alpha\Gamma + P_{Nmax}) - 2kP_{Nmax}}{\sqrt{(\alpha\Gamma + P_{Nmax})^2 - 4k\alpha\Gamma P_{Nmax}}}\right] \quad (7)$$

$$CE_0 = P_N'(C_i = 0) = \alpha \quad (8)$$

$$CE_{\Gamma 0} = |R_p/\Gamma| \quad (9)$$

Γ can be calculated by:

$$\Gamma = \frac{R_p P_{Nmax} - kR_p^2}{\alpha(P_{Nmax} - R_p)} \quad (10)$$

where the line y = $P_{Nmax}$ intersects the approximately straight line of $CO_2$-response curve when $C_i$ is below 200 µmol mol$^{-1}$, and the value of the intersected point on the $x$-axis is $C_{isat}$ (Ye 2010).

**The exponential equation** is expressed as follows (Watling *et al.* 2000):

$$P_N(C_i) = P_{Nmax}(1 - e^{-\alpha C_i/P_{Nmax}} - R_p) \quad (11)$$

where the definitions of all parameters are the same as above.

$CE_\Gamma$, $CE_0$, and $CE_{\Gamma 0}$ are as follows:

$$CE_\Gamma = P_N'(C_i = \Gamma) = \alpha e^{-\alpha C_i/P_{Nmax}} \quad (12)$$

$$CE_0 = P_N'(C_i = 0) = \alpha \quad (13)$$

$$CE_{\Gamma 0} = |R_p/\Gamma| \quad (14)$$

Γ can be calculated by:

$$\Gamma = \frac{P_{Nmax}}{-\alpha} \ln \frac{P_{Nmax} - R_p}{P_{Nmax}} \quad (15)$$

where the line y = $P_{Nmax}$ intersects with the approximately straight line of $CO_2$-response curve at $C_i \leq 200$ µmol mol$^{-1}$, and the value of the intersected point on the $x$-axis is $C_{isat}$ (Dong *et al.* 2007).

**The modified rectangular hyperbola model** is expressed as follows (Ye and Gao 2009, Ye 2010):

$$P_N(C_i) = \alpha \frac{1 - bC_i}{1 + cC_i} C_i - R_p \quad (16)$$

where $b$ and $c$ are coefficients; the definitions of other parameters are the same as above.

$CE_\Gamma$, $CE_0$, and $CE_{\Gamma 0}$ are as follows:

$$CE_\Gamma = P_N'(C_i = \Gamma) = \alpha \frac{1 + (c - b)\, C_i - bcC_i^2}{(1 + cC_i)^2} \quad (17)$$

$$CE_0 = P_N'(C_i = 0) = \alpha \quad (18)$$

$$CE_{\Gamma 0} = |R_p/\Gamma| \quad (19)$$

$C_{isat}$ and $P_{Nmax}$ can be calculated by:

$$C_{isat} = \frac{\sqrt{(b+c)/b} - 1}{c} \quad (20)$$

$$P_{Nmax} = \alpha \left( \frac{\sqrt{b+c} - \sqrt{b}}{c} \right)^2 - R_p \quad (21)$$

## Results

**Photosynthetic $CO_2$ response**: Soil moisture significantly affected the photosynthetic $CO_2$ response of two species (Fig. 1). Under different soil moisture conditions, $P_N$ increased rapidly as $C_i$ increased when $C_i$ was below ~ 200 µmol mol$^{-1}$, then $P_N$ increased slowly when $C_i$ was from ~ 200 µmol mol$^{-1}$ to saturation, and the maximum $P_{Nmax}$ appeared at the $CO_2$-saturation point. $CO_2$ response showed obvious differences when $C_i$ was at saturation under different soil water conditions (Table 1). When RWCs ranged from 46.5 to 81.6% for *P. sibirica*, and 35.4 to 84.5% for *P. tabulaeformis*, $P_N$ of each $CO_2$-response curve of two species changed slightly as $C_i$ increased after $C_i$ reached the $CO_2$-saturation point. When RWCs was out of the above ranges, $P_N$ decreased considerably with increase of $C_i$ after $C_i$ reached saturation; $P_N$ in each curve at the highest $C_i$ was significantly smaller than its $P_{Nmax}$ under the same soil moisture conditions. Clearly, $CO_2$-saturated inhibition occurred. Furthermore, the $CO_2$ responses to soil moisture showed an obvious RWCs threshold. The overall level of $P_N$ in each $CO_2$-response curve increased initially and then decreased as RWCs decreased. The $P_N$ was the highest when RWCs of *P. sibirica* was 66.8%, and that of *P. tabulaeformis* was 73.7%; thus, an increase or decrease in RWCs led to a decrease in the overall $P_N$. $P_{Nmax}$ and $C_{isat}$ were high and $P_N$ did not decrease at high $CO_2$ concentrations when RWCs of *P. sibirica* ranged from 46.5 to 81.6%, and 35.4 to 84.5% for *P. tabulaeformis*; thus, these RWCs ranges were considered suitable for photosynthesis of both species.

**Simulation of $CO_2$-response curves and characteristic parameters**: The simulated effects of the four models fitting the $CO_2$-response data were notably different under different soil moisture conditions (Tables 2, 3). $CO_2$-response curves were well simulated by the four models, and the determination coefficients were all > 0.991 when RWCs was within the appropriate ranges of photosynthesis, *i.e.*, 46.5 to 81.6% for *P. sibirica*, and 35.4 to 84.5% for *P. tabulaeformis*. Moreover, within the above RWCs ranges, only the modified rectangular hyperbola model fitted $P_{Nmax}$ and $C_{isat}$ well, which were closer to the measured value. The $P_{Nmax}$ values fitted by the other three models were significantly higher than their observed values, while the fitted values of $C_{isat}$ were significantly lower than their observed values. When RWCs exceeded the suitable ranges, $P_N$, $P_{Nmax}$, and $C_{isat}$ of the two species decreased, only the modified rectangular hyperbola model could accurately simulate the $CO_2$-response curves ($R^2 > 0.992$) and characteristic parameters.

## Discussion

Water deficit is the main constraint factor for vegetation reconstruction and ecological restoration in the loess, hilly-gully region of China. RWCs not only seriously affects the light-response curves and photosynthetic parameters, but also profoundly affects the $CO_2$-response curves and physiological parameters (Wang *et al.* 2017). The classical form of $CO_2$-response curves can be summarized in three stages (Chen *et al.* 2006, Kathilankal *et al.* 2011). First, an approximately linear segment is observed when $C_i \leq 200$ µmol mol$^{-1}$. Thus, $P_N$ increases rapidly as $C_i$ increases, the slope of the straight line is CE, which reflects the assimilative capacity of plant responses to low $CO_2$ (Wang *et al.* 2010, Ye *et al.* 2017). Second, the curved segment is observed when $C_i$ is from ~ 200 µmol mol$^{-1}$ to saturation, and $P_N$ increases slowly as $C_i$ increases.

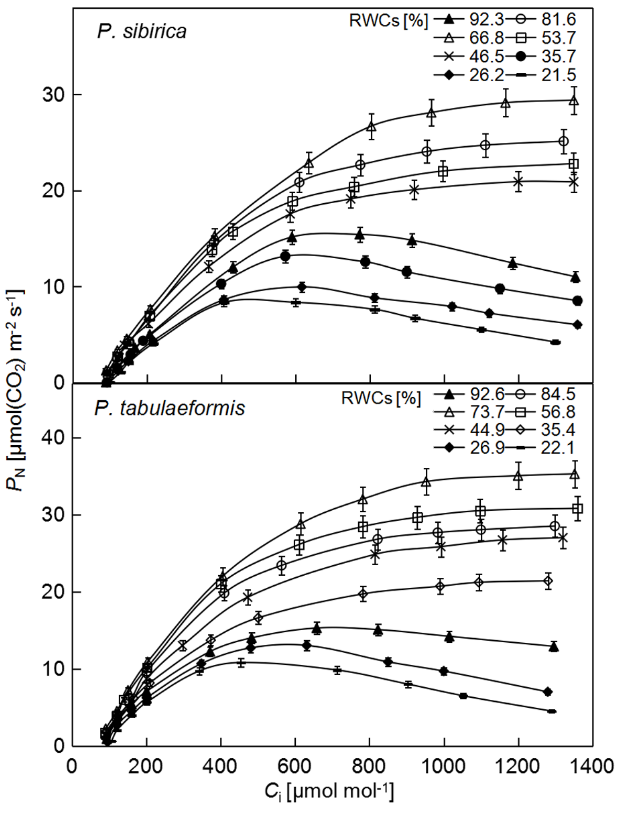


Fig. 1. Photosynthetic $CO_2$ response of *Prunus sibirica* and *Pinus tabulaeformis* under different soil water conditions. Values are means ± SD ($n$ = 3). $C_i$ – intercellular $CO_2$ concentration; $P_N$ – net photosynthetic rate; RWCs – relative soil water content.

Table 1. Photosynthetic $CO_2$-response parameters of two species under different soil water conditions. Values are means ± SD ($n$ = 3). *Different small letters* following each value within a line indicate significant differences at $p$<0.05. $CE_0$ – carboxylation efficiency at $C_i$ = 0; $CE_\Gamma$ – carboxylation efficiency at $C_i = \Gamma$; $CE_{\Gamma 0}$ – slope of the line between $C_i$ = 0 and $C_i = \Gamma$; $C_{isat}$ – $CO_2$-saturation point; Γ – $CO_2$-compensation point; $P_{Nmax}$ – maximum net photosynthetic rate; $R_p$ – photorespiration rate; RWCs – relative soil water content.

| Tree species | $CO_2$-response parameter | Measured value | | | | | | | |
|---|---|---|---|---|---|---|---|---|---|
| *P. sibirica* | RWCs [%] | 92.3 | 81.6 | 66.8 | 53.7 | 46.5 | 35.7 | 26.2 | 21.5 |
| | $CE_0$ [mol m$^{-2}$ s$^{-1}$] | 0.0395$^{d}$ | 0.0461$^{b}$ | 0.0537$^{a}$ | 0.0482$^{b}$ | 0.0436$^{c}$ | 0.0369$^{e}$ | 0.0353$^{e}$ | 0.0294$^{f}$ |
| | $CE_\Gamma$ [mol m$^{-2}$ s$^{-1}$] | 0.0367$^{d}$ | 0.0423$^{c}$ | 0.0504$^{a}$ | 0.0452$^{b}$ | 0.0402$^{c}$ | 0.0337$^{d}$ | 0.0318$^{d}$ | 0.0259$^{e}$ |
| | $CE_{\Gamma 0}$ [mol m$^{-2}$ s$^{-1}$] | 0.0382$^{d}$ | 0.0447$^{b}$ | 0.0522$^{a}$ | 0.0467$^{b}$ | 0.0415$^{c}$ | 0.0355$^{e}$ | 0.0336$^{e}$ | 0.0271$^{f}$ |
| | $C_{isat}$ [μmol mol$^{-1}$] | 690$^{d}$ | 1011$^{b}$ | 1166$^{a}$ | 996$^{b}$ | 920$^{c}$ | 600$^{e}$ | 550$^{f}$ | 500$^{g}$ |
| | $P_{Nmax}$ [μmol($CO_2$) m$^{-2}$ s$^{-1}$] | 15.4$^{d}$ | 25.1$^{b}$ | 29.8$^{a}$ | 22.7$^{c}$ | 20.9$^{c}$ | 13.3$^{d}$ | 9.6$^{e}$ | 8.5$^{e}$ |
| | Γ [μmol mol$^{-1}$] | 90$^{b}$ | 83$^{a}$ | 79$^{a}$ | 81$^{a}$ | 85$^{a}$ | 92$^{b}$ | 95$^{c}$ | 100$^{d}$ |
| | $R_p$ [μmol m$^{-2}$ s$^{-1}$] | 3.44$^{c}$ | 3.71$^{b}$ | 4.12$^{a}$ | 3.78$^{b}$ | 3.53$^{c}$ | 3.27$^{d}$ | 3.19$^{d}$ | 2.71$^{e}$ |
| *P. tabulaeformis* | RWCs [%] | 92.6 | 84.5 | 73.7 | 56.8 | 44.9 | 35.4 | 26.9 | 22.1 |
| | $CE_0$ [mol m$^{-2}$ s$^{-1}$] | 0.0449$^{d}$ | 0.0578$^{b}$ | 0.0658$^{a}$ | 0.0617$^{b}$ | 0.0565$^{b}$ | 0.0493$^{c}$ | 0.0421$^{d}$ | 0.0343$^{e}$ |
| | $CE_\Gamma$ [mol m$^{-2}$ s$^{-1}$] | 0.0425$^{d}$ | 0.0557$^{b}$ | 0.0632$^{a}$ | 0.0577$^{b}$ | 0.0541$^{b}$ | 0.0476$^{c}$ | 0.0394$^{e}$ | 0.0306$^{f}$ |
| | $CE_{\Gamma 0}$ [mol m$^{-2}$ s$^{-1}$] | 0.0438$^{d}$ | 0.0568$^{b}$ | 0.0647$^{a}$ | 0.0595$^{b}$ | 0.0554$^{b}$ | 0.0484$^{c}$ | 0.0407$^{d}$ | 0.0323$^{e}$ |
| | $C_{isat}$ [μmol mol$^{-1}$] | 658$^{c}$ | 1090$^{b}$ | 1200$^{a}$ | 1100$^{b}$ | 995$^{b}$ | 990$^{b}$ | 631$^{c}$ | 600$^{d}$ |
| | $P_{Nmax}$ [μmol($CO_2$) m$^{-2}$ s$^{-1}$] | 15.3$^{d}$ | 28.1$^{b}$ | 35.2$^{a}$ | 29.4b | 27$^{b}$ | 20.3$^{c}$ | 12.9$^{d}$ | 9.8$^{e}$ |
| | Γ [μmol mol$^{-1}$] | 85$^{c}$ | 75$^{a}$ | 70$^{a}$ | 73$^{a}$ | 76$^{a}$ | 80$^{b}$ | 90$^{d}$ | 105$^{e}$ |
| | $R_p$ [μmol m$^{-2}$ s$^{-1}$] | 3.72$^{c}$ | 4.26$^{b}$ | 4.53$^{a}$ | 4.34$^{b}$ | 4.21$^{b}$ | 3.87$^{c}$ | 3.66$^{c}$ | 3.39$^{d}$ |

Third, the almost linear segment when $C_i$ reaches its saturation point, $P_N$ changes insignificantly with the increase of $C_i$, photosynthetic rate at this stage reaches $P_{Nmax}$, which reflects photosynthetic electron transfer rate and photophosphorylation activity (Xu 2013, Ye *et al.* 2018).

The form of $CO_2$-response curves changes when plants encounter stressful conditions, such as drought. However, the quantitative relationship between this change and soil moisture has remained unclear. This study demonstrated that $CO_2$-response curves of two species exhibited a classical shape, with $P_{Nmax}$, CE, $C_{isat}$, and $R_p$ being high and Γ being low within the suitable RWCs range (*i.e.*, 46.5–81.6% for *P. sibirica*, and 35.4–84.5% for *P. tabulaeformis*); $P_N$ values were the highest when RWCs of *P. sibirica* was 66.8%, and that of *P. tabulaeformis* was 73.7%. Three photosynthetic parameters, $P_{Nmax}$, CE, and $C_{isat}$, declined dramatically when the soil moisture content exceeded the above ranges. Two species exhibited wide photosynthetic adaptability to soil moisture compared to the suitable RWCs ranges of *Robinia pseudoacacia* L. (50.0–81.6%), *Platycladus orientalis* L. (45.3–75.0%) (Zhang *et al.* 2003), *Syringa oblata* Lindl. (58.8–76.6%) (Chen *et al.* 2004), and *Ziziphus jujube* (46.0–80.5%) (Yang *et al.* 2018).

CE is usually obtained by a traditional linear regression method, whereby CE is the slope of the straight line of $CO_2$-response curve at a low $CO_2$ concentration ($C_i \leq$ ~ 200 μmol mol$^{-1}$) (Xu 2013, Kang *et al.* 2014). CE values of different plants vary greatly (Yiotis and Manetas 2010, Feng and Dietze 2013, Zhao *et al.* 2017). Although Hu *et al.* (2008) showed that soil moisture greatly affected the CE values of plants, the quantitative relationship between CE and soil moisture has remained unclear. According to previous studies, $CO_2$-response curve does not have a strictly linear relationship at the low $CO_2$ concentration (Ye and Gao 2008, Ye and Yu 2009).

$CO_2$-response models are mainly used to fit the process of $CO_2$ response and its characteristic parameters to extract the variables with specific physiological meaning; these parameters can be used to describe the physiological response of leaves to different treatments (Zeng *et al.* 2010, Bernacchi *et al.* 2013). For example, $CE_\Gamma$, the carboxylation efficiency at the $CO_2$-compensation point, $CE_0$, the carboxylation efficiency when the $CO_2$ concentration is 0, $CE_{\Gamma 0}$, the absolute value of the slope of the line between $C_i$ = 0 and $C_i = \Gamma$ can be fitted, and they have clear physiological meanings and unique values. However, the applicability and simulated effect of the empirical models are limited by their asymptotic form with no extreme values (Ye and Gao 2009, Ye 2010). Simulated $P_{Nmax}$ was much larger than the measured values, while simulated $C_{isat}$ was far lower than the measured values (Ye and Gao 2008, Jiao and Wei 2010, Lv *et al.* 2016). The same problem was noted in this study.

Although the modified rectangular hyperbola model proposed in recent years can fit and analyze various forms of $CO_2$-response curves more accurately (Lv *et al.* 2016, Ye *et al.* 2017), overcoming the limitations of other models to a certain extent, there are few reports regarding its application in plants under different soil moisture conditions. This study indicated that when the soil moisture was within a suitable RWCs range, the $CO_2$-response curves and characteristic parameters were well fitted by the four models ($R^2$ > 0.991), where the nonrectangular hyperbola model and modified rectangular hyperbola model fit the data better than the other two models. When soil moisture was too high or too low, only the modified rectangular hyperbola model was obviously better than the

Table 2. Photosynthetic $CO_2$-response parameters of *Prunus sibirica* fitted by four models under different soil water conditions. Values are means ± SD ($n$ = 3). $CE_0$ – carboxylation efficiency at $C_i = 0$; $CE_\Gamma$ – carboxylation efficiency at $C_i = \Gamma$; $CE_{\Gamma 0}$ – slope of the line between $C_i = 0$ and $C_i = \Gamma$; $C_{isat}$ – $CO_2$-saturation point; $\Gamma$ – $CO_2$-compensation point; $P_{Nmax}$ – maximum net photosynthetic rate; $R_p$ – photorespiration rate; RWCs – relative soil water content.

| $CO_2$-response model | $CO_2$-response parameter | RWCs [%] | | | | | | | |
|---|---|---|---|---|---|---|---|---|---|
| | | 92.3 | 81.6 | 66.8 | 53.7 | 46.5 | 35.7 | 26.2 | 21.5 |
| Rectangular hyperbola model | $CE_0$ [mol m$^{-2}$ s$^{-1}$] | 0.0509 | 0.0485 | 0.0562 | 0.0511 | 0.0472 | 0.0452 | - | - |
| | $CE_\Gamma$ [mol m$^{-2}$ s$^{-1}$] | 0.0483 | 0.0459 | 0.0534 | 0.0478 | 0.0448 | 0.0417 | - | - |
| | $CE_{\Gamma 0}$ [mol m$^{-2}$ s$^{-1}$] | 0.0496 | 0.0471 | 0.0551 | 0.0493 | 0.0455 | 0.0435 | - | - |
| | $C_{isat}$ [μmol mol$^{-1}$] | 464 | 473 | 487 | 445 | 434 | 378 | - | - |
| | $P_{Nmax}$ [μmol($CO_2$) m$^{-2}$ s$^{-1}$] | 32.94 | 37.61 | 45.81 | 33.64 | 30.3 | 18.45 | - | - |
| | $\Gamma$ [μmol mol$^{-1}$] | 81.85 | 80.84 | 75.61 | 78.73 | 81.5 | 83.86 | - | - |
| | $R_p$ [μmol m$^{-2}$ s$^{-1}$] | 4.06 | 3.81 | 4.17 | 3.88 | 3.71 | 3.65 | - | - |
| | determination coefficient $R^2$ | 0.804 | 0.991 | 0.992 | 0.995 | 0.993 | 0.816 | - | - |
| Nonrectangular hyperbola model | $CE_0$ [mol m$^{-2}$ s$^{-1}$] | 0.0468 | 0.0472 | 0.0546 | 0.0521 | 0.0481 | 0.0474 | - | - |
| | $CE_\Gamma$ [mol m$^{-2}$ s$^{-1}$] | 0.0433 | 0.0435 | 0.0515 | 0.0457 | 0.0437 | 0.0442 | - | - |
| | $CE_{\Gamma 0}$ [mol m$^{-2}$ s$^{-1}$] | 0.0450 | 0.0459 | 0.0534 | 0.0476 | 0.0441 | 0.0460 | - | - |
| | $C_{isat}$ [μmol mol$^{-1}$] | 539 | 596 | 610 | 585 | 571 | 445 | - | - |
| | $P_{Nmax}$ [μmol($CO_2$) m$^{-2}$ s$^{-1}$] | 25.21 | 38.97 | 40.46 | 34.21 | 30.36 | 21.08 | - | - |
| | $\Gamma$ [μmol mol$^{-1}$] | 84.04 | 82.03 | 77.97 | 78.9 | 83.34 | 87.37 | - | - |
| | $R_p$ [μmol m$^{-2}$ s$^{-1}$] | 3.78 | 3.77 | 4.16 | 3.76 | 3.67 | 4.02 | - | - |
| | determination coefficient $R^2$ | 0.885 | 0.998 | 0.999 | 0.998 | 0.998 | 0.892 | - | - |
| Exponential equation | $CE_0$ [mol m$^{-2}$ s$^{-1}$] | 0.0496 | 0.0478 | 0.0562 | 0.0499 | 0.0461 | 0.0445 | 0.0439 | 0.0434 |
| | $CE_\Gamma$ [mol m$^{-2}$ s$^{-1}$] | 0.0469 | 0.0436 | 0.0531 | 0.0467 | 0.0435 | 0.0415 | 0.0401 | 0.0387 |
| | $CE_{\Gamma 0}$ [mol m$^{-2}$ s$^{-1}$] | 0.0472 | 0.0465 | 0.0544 | 0.0486 | 0.0447 | 0.0423 | 0.0412 | 0.0403 |
| | $C_{isat}$ [μmol mol$^{-1}$] | 495 | 550 | 605 | 535 | 520 | 517 | 309 | 301 |
| | $P_{Nmax}$ [μmol($CO_2$) m$^{-2}$ s$^{-1}$] | 25. 68 | 37.11 | 45.17 | 33.65 | 29.97 | 23.67 | 21.58 | 19.67 |
| | $\Gamma$ [μmol mol$^{-1}$] | 82.76 | 81.54 | 76.79 | 78.82 | 82.28 | 87.9 | 89.6 | 88.93 |
| | $R_p$ [μmol m$^{-2}$ s$^{-1}$] | 3.91 | 3.79 | 4.18 | 3.83 | 3.67 | 3.72 | 3.69 | 3.58 |
| | determination coefficient $R^2$ | 0.845 | 0.996 | 0.996 | 0.998 | 0.996 | 0.853 | 0.725 | 0.609 |
| Modified rectangular hyperbola model | $CE_0$ [mol m$^{-2}$ s$^{-1}$] | 0.0437 | 0.0468 | 0.0547 | 0.0492 | 0.0459 | 0.0392 | 0.0373 | 0.0317 |
| | $CE_\Gamma$ [mol m$^{-2}$ s$^{-1}$] | 0.0401 | 0.0436 | 0.0523 | 0.0469 | 0.0423 | 0.0341 | 0.0338 | 0.0292 |
| | $CE_{\Gamma 0}$ [mol m$^{-2}$ s$^{-1}$] | 0.0412 | 0.0455 | 0.0531 | 0.0479 | 0.0432 | 0.0374 | 0.0357 | 0.0305 |
| | $C_{isat}$ [μmol mol$^{-1}$] | 685 | 1118 | 1178 | 994 | 935 | 614 | 539 | 513 |
| | $P_{Nmax}$ [μmol($CO_2$) m$^{-2}$ s$^{-1}$] | 15.69 | 24.96 | 29.98 | 22.8 | 20.37 | 13.51 | 10.38 | 9.13 |
| | $\Gamma$ [μmol mol$^{-1}$] | 88.14 | 82.46 | 80.34 | 79.88 | 87.55 | 90.42 | 93.12 | 102.69 |
| | $R_p$ [μmol m$^{-2}$ s$^{-1}$] | 3.63 | 3.75 | 4.27 | 3.82 | 3.78 | 3.38 | 3.32 | 3.13 |
| | determination coefficient $R^2$ | 0.995 | 0.999 | 0.999 | 0.999 | 0.998 | 0.996 | 0.993 | 0.992 |

other three models fitting the $CO_2$-response process and its characteristic parameters in the leaves of two species.

**Conclusions**: This study indicated that soil moisture content affected the $CO_2$-response process in the leaves of two species. The photosynthetic $CO_2$-response curves presented classical form when the RWCs ranged from 46.5 to 81.6% for *P. sibirica*, and 35.4 to 84.5% for *P. tabulaeformis*, photosynthetic efficiency and the $P_N$ were the highest when RWCs of *P. sibirica* was ~ 66.8%, and that of *P. tabulaeformis* was ~ 73.7%. Three photosynthetic parameters, $P_{Nmax}$, CE, and $C_{isat}$, declined dramatically when the soil moisture exceeded the suitable water ranges for photosynthesis of the two species. Thus, the suitable RWCs was 46.5 to 81.6% for *P. sibirica*, and 35.4 to 84.5% for *P. tabulaeformis*, and the most suitable RWCs was ~ 66.8% for *P. sibirica*, and ~ 73.7% for *P. tabulaeformis*.

The CE values of *P. sibirica* and *P. tabulaeformis* were significantly different under different soil moisture conditions. $CE_{\Gamma 0}$ of *P. sibirica* ranged from 0.0271 to 0.0522, with a comparatively higher value in the RWCs range of 46.5–81.6%; the maximum appeared when RWCs was ~ 66.8%; $CE_{\Gamma 0}$ of *P. tabulaeformis* ranged from 0.0323 to 0.0647, with a comparatively higher value in the RWCs range of 35.4–84.5%, the maximum appeared when RWCs was ~ 73.7%. The results of this study showed that the CE values of two species had obvious threshold responses to soil moisture.

When soil moisture was within the suitable RWCs range, the $CO_2$-response curves and characteristic para-

Table 3. Photosynthetic $CO_2$-response parameters of *Pinus tabulaeformis* fitted by four models under different soil water conditions. Values are means ± SD ($n$ = 3). $CE_0$ – carboxylation efficiency at $C_i = 0$; $CE_\Gamma$ – carboxylation efficiency at $C_i = \Gamma$; $CE_{\Gamma 0}$ – slope of the line between $C_i = 0$ and $C_i = \Gamma$; $C_{isat}$ – $CO_2$-saturation point; Γ – $CO_2$-compensation point; $P_{Nmax}$ – maximum net photosynthetic rate; $R_p$ – photorespiration rate; RWCs – relative soil water content.

| $CO_2$-response model | $CO_2$-response parameter | RWCs [%] 92.6 | 84.5 | 73.7 | 56.8 | 44.9 | 35.4 | 26.9 | 22.1 |
|---|---|---|---|---|---|---|---|---|---|
| Rectangular hyperbola model | $CE_0$ [mol $m^{-2}$ $s^{-1}$] | 0.0583 | 0.0619 | 0.0717 | 0.0656 | 0.0611 | 0.0562 | - | - |
| | $CE_\Gamma$ [mol $m^{-2}$ $s^{-1}$] | 0.0552 | 0.0587 | 0.0679 | 0.0623 | 0.0586 | 0.0535 | - | - |
| | $CE_{\Gamma 0}$ [mol $m^{-2}$ $s^{-1}$] | 0.0568 | 0.0606 | 0.0695 | 0.0644 | 0.0605 | 0.0551 | - | - |
| | $C_{isat}$ [μmol $mol^{-1}$] | 390 | 525 | 548 | 532 | 523 | 515 | - | - |
| | $P_{Nmax}$ [μmol($CO_2$) $m^{-2}$ $s^{-1}$] | 24.13 | 38.48 | 52.23 | 43.33 | 40.91 | 31.79 | - | - |
| | Γ [μmol $mol^{-1}$] | 76.78 | 72.32 | 67.21 | 70.04 | 73.53 | 76.07 | - | - |
| | $R_p$ [μmol $m^{-2}$ $s^{-1}$] | 4.36 | 4.38 | 4.67 | 4.51 | 4.45 | 4.19 | - | - |
| | determination coefficient $R^2$ | 0.839 | 0.998 | 0.991 | 0.993 | 0.996 | 0.996 | - | - |
| Nonrectangular hyperbola model | $CE_0$ [mol $m^{-2}$ $s^{-1}$] | 0.0473 | 0.0558 | 0.0672 | 0.0564 | 0.0517 | 0.0452 | - | - |
| | $CE_\Gamma$ [mol $m^{-2}$ $s^{-1}$] | 0.0431 | 0.0519 | 0.0632 | 0.0531 | 0.0482 | 0.0414 | - | - |
| | $CE_{\Gamma 0}$ [mol $m^{-2}$ $s^{-1}$] | 0.0465 | 0.0536 | 0.0658 | 0.0543 | 0.0497 | 0.0423 | - | - |
| | $C_{isat}$ [μmol $mol^{-1}$] | 542 | 570 | 693 | 661 | 650 | 602 | - | - |
| | $P_{Nmax}$ [μmol($CO_2$) $m^{-2}$ $s^{-1}$] | 35.77 | 44.75 | 58.29 | 56.73 | 50.36 | 41.27 | - | - |
| | Γ [μmol $mol^{-1}$] | 92.06 | 79.07 | 70.38 | 80.35 | 86.94 | 93.4 | - | - |
| | $R_p$ [μmol $m^{-2}$ $s^{-1}$] | 4.28 | 4.24 | 4.63 | 4.36 | 4.32 | 3.95 | - | - |
| | determination coefficient $R^2$ | 0.881 | 0.999 | 0.999 | 0.999 | 0.998 | 0.999 | - | - |
| Exponential equation | $CE_0$ [mol $m^{-2}$ $s^{-1}$] | 0.0569 | 0.0605 | 0.0698 | 0.0632 | 0.0597 | 0.0532 | 0.0555 | 0.0538 |
| | $CE_\Gamma$ [mol $m^{-2}$ $s^{-1}$] | 0.0541 | 0.0567 | 0.0661 | 0.0604 | 0.0572 | 0.0509 | 0.0522 | 0.0513 |
| | $CE_{\Gamma 0}$ [mol $m^{-2}$ $s^{-1}$] | 0.0557 | 0.0589 | 0.0685 | 0.0617 | 0.0585 | 0.0520 | 0.0531 | 0.0524 |
| | $C_{isat}$ [μmol $mol^{-1}$] | 321 | 438 | 452 | 426 | 435 | 441 | 276 | 266 |
| | $P_{Nmax}$ [μmol($CO_2$) $m^{-2}$ $s^{-1}$] | 27.26 | 35.39 | 40.87 | 34.14 | 34.15 | 33.92 | 25.79 | 22.85 |
| | Γ [μmol $mol^{-1}$] | 80.49 | 73.99 | 68.16 | 71.83 | 73.65 | 77.92 | 82.63 | 93.84 |
| | $R_p$ [μmol $m^{-2}$ $s^{-1}$] | 4.48 | 4.36 | 4.67 | 4.43 | 4.31 | 4.05 | 4.39 | 4.92 |
| | determination coefficient $R^2$ | 0.769 | 0.998 | 0.998 | 0.997 | 0.998 | 0.995 | 0.731 | 0.552 |
| Modified rectangular hyperbola model | $CE_0$ [mol $m^{-2}$ $s^{-1}$] | 0.0473 | 0.0596 | 0.0692 | 0.0625 | 0.0583 | 0.0512 | 0.0448 | 0.0355 |
| | $CE_\Gamma$ [mol $m^{-2}$ $s^{-1}$] | 0.0428 | 0.0561 | 0.0646 | 0.0592 | 0.0551 | 0.0481 | 0.0416 | 0.0312 |
| | $CE_{\Gamma 0}$ [mol $m^{-2}$ $s^{-1}$] | 0.0452 | 0.0579 | 0.0668 | 0.0601 | 0.0569 | 0.0494 | 0.0434 | 0.0331 |
| | $C_{isat}$ [μmol $mol^{-1}$] | 559 | 1056 | 1196 | 1097 | 990 | 873 | 497 | 463 |
| | $P_{Nmax}$ [μmol($CO_2$) $m^{-2}$ $s^{-1}$] | 17.47 | 26.98 | 35.64 | 29.66 | 28.07 | 25.15 | 14.2 | 12.39 |
| | Γ [μmol $mol^{-1}$] | 84.59 | 74.11 | 69.34 | 72.99 | 74.75 | 79.29 | 86.44 | 106.86 |
| | $R_p$ [μmol $m^{-2}$ $s^{-1}$] | 3.82 | 4.29 | 4.63 | 4.39 | 4.25 | 3.92 | 3.75 | 3.54 |
| | determination coefficient $R^2$ | 0.998 | 0.999 | 0.999 | 0.999 | 0.999 | 0.999 | 0.994 | 0.995 |

meters were well fitted by the four models. The nonrectangular hyperbola model and modified rectangular hyperbola model were better than the other two models. However, when soil moisture exceeded the suitable RWCs ranges, only the modified rectangular hyperbola model fit the $CO_2$-response curves and photosynthetic parameters accurately. Compared to the other three models, the modified rectangular hyperbola model demonstrated extensive applicability for fitting photosynthetic $CO_2$-response process under different soil moisture conditions.

## References


Ali A.A., Xu C., Rogers A. *et al.*: A global scale mechanistic model of photosynthetic capacity (LUNAV1.0). – Geosci. Model Dev. **9**: 587-606, 2016.

Baly E.C.: The kinetics of photosynthesis. – P. Roy. Soc. Lond. B Bio. **117**: 218-239, 1935.

Bao H.: [Response growth characteristics of *Prunus ansu* from different provenances in seedling stage to drought stress.] – J. Inner Mong. For. Sci. Technol. **41**: 5-8, 2015. [In Chinese]

Bellasio C.: A generalised dynamic model of leaf-level $C_3$ photosynthesis combining light and dark reactions with stomatal behaviour. – Photosynth. Res. **141**: 99-118, 2019.

Bellasio C., Quirk J., Beerling D.J.: Stomatal and non-stomatal limitations in savanna trees and $C_4$ grasses grown at low, ambient and high atmospheric $CO_2$. – Plant Sci. **274**: 181-192, 2018.

Bernacchi C.J., Bagley J.E., Serbin S.P. *et al.*: Modelling $C_3$ photosynthesis from the chloroplast to the ecosystem. – Plant Cell Environ. **36**: 1641-1657, 2013.

Bhusal N., Han S.G., Yoon T.M.: Impact of drought stress on photosynthetic response, leaf water potential, and stem sap flow in two cultivars of bi-leader apple trees (*Malus × domestica* Borkh.). – Sci. Hortic.-Amsterdam **246**: 535-543, 2019.

Brito C., Dinis L.T., Moutinho-Pereira J. *et al.*: Drought stress effects and olive tree acclimation under a changing climate. – Plants **8**: 232-252, 2019.

Chen G.Y., Yu G.L., Chen Y. *et al.*: [Exploring the observation methods of photosynthetic responses to light and carbon dioxide.] – J. Plant Psychophysiol. Mol. Biol. **32**: 691-696, 2006. [In Chinese]

Chen X.J., Zhang G.C., Liu X. *et al.*: [Diurnal variations and response to light of gas exchange parameters of clove (*Syringa oblata* Lindl.) leaf in loess hilly region.] – Sci. Soil Water Conserv. **2**: 102-107, 2004. [In Chinese]

Davidson A.M., Da Silva D., Saa S. *et al.*: The influence of elevated $CO_2$ on the photosynthesis, carbohydrate status, and plastochron of young peach (*Prunus persica*) trees. – Hortic. Environ. Biote. **57**: 364-370, 2016.

Dong Z.X., Han Q.F., Jia Z.K. *et al.*: [Photosynthesis rate in response to light intensity and $CO_2$ concentration in different alfalfa varieties.] – Acta Ecol. Sin. **27**: 2272-2278, 2007. [In Chinese]

Drake J.E., Power S.A., Duursma R.A. *et al.*: Stomatal and non-stomatal limitations of photosynthesis for four tree species under drought: a comparison of model formulations. – Agr. Forest Meteorol. **247**: 454-466, 2017.

Dubois J.J.B., Fiscus E.L., Booker F.L. *et al.*: Optimizing the statistical estimation of the parameters of the Farquhar-von Caemmerer-Berry model of photosynthesis. – New Phytol. **176**: 402-414, 2007.

Ellsworth D.S., Crous K.Y., Lambers H., Cooke J.: Phosphorus recycling in photorespiration maintains high photosynthetic capacity in woody species. – Plant Cell Environ. **38**: 1142-1156, 2015.

Falqueto A.R., da Silva Júnior R.A., Gomes M.T.G. *et al.*: Effects of drought stress on chlorophyll *a* fluorescence in two rubber tree clones. – Sci. Hortic.-Amsterdam **224**: 238-243, 2017.

Farquhar G.D., von Caemmerer S., Berry J.A.: A biochemical model of photosynthetic $CO_2$ assimilation in leaves of $C_3$ species. – Planta **149**: 78-90, 1980.

Feng X., Dietze M.: Scale dependence in the effects of leaf ecophysiological traits on photosynthesis: Bayesian parameterization of photosynthesis models. – New Phytol. **200**: 1132-1144, 2013.

Groenendijk M., Dolman A.J., van der Molen M.K. *et al.*: Assessing parameter variability in a photosynthesis model within and between plant functional types using global Fluxnet eddy covariance data. – Agr. Forest Meteorol. **151**: 22-38, 2011.

Guan J., Wang J., Lv X.: $P_n$-PAR and $CO_2$ responses of *Prunus avium* to drought stress during hard nucleus stage. 7th International Conference on Energy, Environment and Sustainable Development (ICEESD 2018). – Adv. Eng. Res. **163**: 408-411, 2018.

Guo W.X., Zhao Z.J., Zheng J., Li J.Q.: Interaction of soil water and nitrogen on the photosynthesis and growth in *Pinus tabulaeformis* seedlings. – Sci. Silvae Sin. **53**: 37-48, 2017.

Ha R., Ma Y.P., Cao B. *et al.*: [Effects of simulated elevated $CO_2$ concentration on vegetative growth and fruit quality in *Lycium barbarum*.] – Sci. Silvae Sin. **55**: 28-36, 2019. [In Chinese]

Harley P.C., Thomas R.B., Reynolds J.F., Strain B.R.: Modelling photosynthesis of cotton grown in elevated $CO_2$. – Plant Cell Environ. **15**: 271-282, 1992.

Heyam D.: Determination of moisture content and liquid limit of foundations soils, using microwave radiation, in different locations of Sulaimani governorate, Kurdistan region-Iraq. – World Acad. Sci. Ing. Technol. **6**: 544-550, 2012.

Hu W.H., Hu X.H., Zeng J.J. *et al.*: [Effects of drought on photosynthetic characteristics in two pepper cultivars.] – J. Huazhong Agr. Univ. **27**: 776-781, 2008. [In Chinese]

IPCC: Summary for Policymakers. – In: Stocker T.F., Qin D.H., Plattner G.K. *et al.* (ed.): Climate Change 2013: The Physical Science Basis. Contribution of Working Group I to the Fifth Assessment Report of the Intergovernmental Panel on Climate Change. Pp. 3-29. Cambridge University Press, Cambridge-New York 2013.

Jiao Y.M., Wei X.L.: [Application of two photosynthetic light response and $CO_2$ response curve-fitting models on karst species.]– Guizhou Agr. Sci. **4**: 162-167, 2010. [In Chinese]

Jin J.T., Li Y., Li R.J. *et al.*: [Advances in studies on effects of elevated atmospheric carbon dioxide concentration on plant growth and development.] – Plant Physiol. J. **55**: 558-568, 2019. [In Chinese]

Kang H.J., Tao Y.L., Quan W. *et al.*: [Fitting mitochondrial respiration rates under light by photosynthetic $CO_2$ response models.] – Chin. J. Plant Ecol. **38**: 1356-1363, 2014. [In Chinese]

Karimi S., Rahemi M., Rostami A.A., Sedaghat S.: Drought effects on growth, water content and osmoprotectants in four olive cultivars with different drought tolerance. – Int. J. Fruit Sci. **18**: 254-267, 2018.

Kathilankal J.C., Mozdzer T.J., Fuentes J.D. *et al.*: Physiological responses of *Spartina alterniflora* to varying environmental conditions in Virginia marshes. – Hydrobiologia **669**: 167, 2011.

King J.L., Edwards G.E., Cousins A.B.: The efficiency of the $CO_2$-concentrating mechanism during single-cell $C_4$ photosynthesis. – Plant Cell Environ. **35**: 513-523, 2012.

Lang Y., Wang M., Zhang G.C., Zhao K.Q.: Experimental and simulated light responses of photosynthesis in leaves of three tree species under different soil water conditions. – Photosynthetica **51**: 370-378, 2013.

Liang X.Y., Liu S.R.: [A review on the FvCB biochemical model of photosynthesis and the measurement of $A$-$C_i$ curve.] – Chin. J. Plant Ecol. **41**: 693-706, 2017. [In Chinese]

Liu J.J., Li J.Y., Zhang J.G.: [Influences of drought stress on photosynthetic characteristics and water use efficiency of 4 tree species under elevated $CO_2$ concentration.] – For. Res. **28**: 339-345, 2015. [In Chinese]

Liu X., Luo G.J.: [Effect of water stress on growth and physiological characteristics in *Quercus acutissima*.] – J. North. Agric. **47**: 11-14, 2019. [In Chinese]

Liu Z.S., Yang W.Y., Yu X.L.: A new predictive model for plants photosynthesis influenced by major climatic conditions. – 2019 IOP Conf. Ser.: Earth Environ. Sci. **291**: 1-7, 2019b.

Liu Z.Y., Ma C.M., Liu C.P. *et al.*: [Construction and validation of water-consumption prediction model for *Prunus sibirica* in the rocky mountainous area of north China.] – J. Centr. South Univ. For. Technol. **39**: 21-27, 2019a. [In Chinese]

Lu S.W., Ding J., Li S.N. *et al.*: [Studies on characteristics of water consumption for transpiration of economic forest tree species.] – J. Henan Agric. Sci. **46**: 113-119, 2017. [In Chinese]

Lv Y., Liu T.X., Yan X. *et al.*: [Response of photosynthetic rate of *Salix gordejevii* and *Caragana microphylla* to light intensity and $CO_2$ concentration in the dune-meadow transitional area of Horqin sandy land.] – Chin. J. Ecol. **36**: 3157-3167, 2016. [In Chinese]

Nickelsen K.: Explaining Photosynthesis: Models of Biochemical Mechanisms. Pp. 220-226. Springer, Dordrecht 2015.

Niinemets Ü., Keenan T.F., Hallik L.: A worldwide analysis of within-canopy variations in leaf structural, chemical and physiological traits across plant functional types. – New Phytol. **205**: 973-993, 2015.
Reich P.B., Sendall K.M., Stefanski A. *et al.*: Effects of climate warming on photosynthesis in boreal tree species depend on soil moisture. – Nature **562**: 263-267, 2018.
Renninger H.J., Carlo N., Clark K.L., Schäfer K.V.: Physiological strategies of co-occurring oaks in a water- and nutrient-limited ecosystem. – Tree Physiol. **34**: 159-173, 2014.
Sharkey T.D.: What gas exchange data can tell us about photosynthesis. – Plant Cell Environ. **39**: 1161-1163, 2016.
Singh S.K., Reddy V.R.: Methods of mesophyll conductance estimation: Its impact on key biochemical parameters and photosynthetic limitations in phosphorus-stressed soybean across $CO_2$. – Physiol. Plantarum **157**: 234-254, 2016.
Sun J.D., Feng Z.Z., Leakey A.D.B. *et al.*: Inconsistency of mesophyll conductance estimate causes the inconsistency for the estimates of maximum rate of Rubisco carboxylation among the linear, rectangular and non-rectangular hyperbola biochemical models of leaf photosynthesis – A case study of $CO_2$ enrichment and leaf aging effects in soybean. – Plant Sci. **226**: 49-60, 2014.
von Caemmerer S.: Steady-state models of photosynthesis. – Plant Cell Environ. **36**: 1617-1630, 2013.
Walker B.J., Orr D.J., Carmo-Silva E. *et al.*: Uncertainty in measurements of the photorespiratory $CO_2$ compensation point and its impact on models of leaf photosynthesis. – Photosynth. Res. **132**: 245-255, 2017.
Wang G.P., Li F., Zhang J. *et al.*: Overaccumulation of glycine betaine enhances tolerance of the photosynthetic apparatus to drought and heat stress in wheat. – Photosynthetica **48**: 30-41, 2010.
Wang H.Z., Han L., Xu Y.L. *et al.*: [Effects of soil water gradient on photosynthetic characteristics and stress resistance of *Populus pruinosa* in the Tarim Basin, China.] – Acta Ecol. Sin. **37**: 432-442, 2017. [In Chinese]
Wang J.L., Yu G.R., Wang B.L. *et al.*: [Response of photosynthetic rate and stomatal conductance of rice to light intensity and $CO_2$ concentration in northern China.] – Acta Phytoecol. Sin. **29**: 16-25, 2005. [In Chinese]
Wang Q., Liu X.M., Wang H.T. *et al.*: [Effects of drought and waterlogging on growth and photosynthesis of potted young *Pinus tabulaeformis* Carr.] – Sci. Soil Water Conserv. **13**: 40-47, 2015. [In Chinese]
Wang Y., Sperry J.S., Venturas M.D. *et al.*: The stomatal response to rising $CO_2$ concentration and drought is predicted by a hydraulic trait-based optimization model. – Tree Physiol. **39**: 1416-1427, 2019.
Wang Z.C., Kang S.Z., Jensen C.R., Liu F.L.: Alternate partial root-zone irrigation reduces bundle-sheath cell leakage to $CO_2$ and enhances photosynthetic capacity in maize leaves. – J. Exp. Bot. **63**: 1145-1153, 2012.
Watling J.R., Press M.C., Quick W.P.: Elevated $CO_2$ induces biochemical and ultrastructural changes in leaves of the $C_4$ cereal sorghum. – Plant Physiol. **123**: 1143-1152, 2000.
Wu X., Tang Y.K., Chen C. *et al.*: [Photosynthesis light response characteristics and environmental adaptability of *Hippophae rhamnoides* L., *Pinus tabulaeformis* and *Robinia pseudoacacia* in the Loess hilly region of China.] – Acta Ecol. Sin. **39**: 8111-8125, 2019. [In Chinese]
Xia X.X., Zhang S.Y., Zhang G.C. *et al.*: [Effects of soil moisture on the photosynthetic light reaction of *Rosa xanthina* L. in a loess hilly region.] – Acta Ecol. Sin. **36**: 5142-5149, 2016. [In Chinese]
Xu D.Q.: [The science of photosynthesis.] Pp. 236-244. Science Press, Beijing 2013. [In Chinese]
Yang R., Lang Y., Zhang G.C. *et al.*: [Responses of photosynthesis and fluorescence of *Ziziphus jujuba* var. *spinosa* to soil drought stress.] – Acta Bot. Bor.-Occident. Sin. **38**: 922-931, 2018. [In Chinese]
Ye Z.P.: [A review on modeling of responses of photosynthesis to light and $CO_2$.] – Chin. J. Plant Ecol. **34**: 727-740, 2010. [In Chinese]
Ye Z.P., Duan S.H., An T. *et al.*: [Construction of $CO_2$-response model of electron transport rate in $C_4$ crop and its application.] – Chin. J. Plant Ecol. **42**: 1000-1008, 2018. [In Chinese]
Ye Z.P., Gao J.: [Change of carboxylation efficiency of *Salvia miltiorrhiza* in the vicinity of $CO_2$ compensation point.] – J. North. Agric. For. Univ. **36**: 160-164, 2008. [In Chinese]
Ye Z.P., Gao J.: [Application of a new model of light-response and $CO_2$-response of photosynthesis in *Salvia miltiorrhiza*.] – J. North. Agric. For. Univ. **37**: 129-134, 2009. [In Chinese]
Ye Z.P., Wang Y.J., Wang L.L. *et al.*: [Response of photorespiration of *Glycine max* leaves to light intensity and $CO_2$ concentration.] – Chin. J. Ecol. **36**: 2535-2541, 2017. [In Chinese]
Ye Z.P., Yu Q.: [A comparison of response curves of winter wheat photosynthesis to flag leaf intercellular and air $CO_2$ concentrations.] – Chin. J. Ecol. **28**: 2233-2238, 2009. [In Chinese]
Yiotis C., Manetas Y.: Sinks for photosynthetic electron flow in green petioles and pedicels of *Zantedeschia aethiopica*: Evidence for innately high photorespiration and cyclic electron flow rates. – Planta **232**: 523-531, 2010.
Zeng W., Zhou G.S., Jia B.R. *et al.*: Comparison of parameters estimated from $A/C_i$ and $A/C_c$ curve analysis. – Photosynthetica **48**: 323-331, 2010.
Zhang G.C., Liu X., He K.N.: [Grading of *Robinia pseudoacacia* and *Platycladus orientalis* woodland soil's water availability and productivity in semi-arid region of Loess Plateau.] – J. Appl. Ecol. **14**: 858-862, 2003. [In Chinese]
Zhao Y.W., Duan S.R., Zheng Y. *et al.*: [Comparison of light response curve and $CO_2$ response curve of *Sophora moorcroftiana* under several photosynthesis models.] – J. Plateau Agric. **1**: 159-165, 2017. [In Chinese]